

Climate sensitivity increases under higher CO₂ levels due to feedback temperature dependence

Article

Accepted Version

Bloch-Johnson, J. ORCID: <https://orcid.org/0000-0002-8465-5383>, Rugenstein, M., Stolpe, M. B., Rohrschneider, T., Zheng, Y. and Gregory, J. M. ORCID: <https://orcid.org/0000-0003-1296-8644> (2021) Climate sensitivity increases under higher CO₂ levels due to feedback temperature dependence. *Geophysical Research Letters*, 48 (4). e2020GL089074. ISSN 0094-8276 doi: 10.1029/2020GL089074 Available at <https://centaur.reading.ac.uk/97773/>

It is advisable to refer to the publisher's version if you intend to cite from the work. See [Guidance on citing](#).

To link to this article DOI: <http://dx.doi.org/10.1029/2020GL089074>

Publisher: American Geophysical Union

All outputs in CentAUR are protected by Intellectual Property Rights law, including copyright law. Copyright and IPR is retained by the creators or other copyright holders. Terms and conditions for use of this material are defined in the [End User Agreement](#).

www.reading.ac.uk/centaur

CentAUR

Central Archive at the University of Reading

Reading's research outputs online

1 **Climate sensitivity increases under higher CO₂ levels**
2 **due to feedback temperature dependence**

3 **Jonah Bloch-Johnson¹, Maria Rugenstein^{2,3}, Martin B. Stolpe, Tim**
4 **Rohrschneider², Yiyu Zheng², and Jonathan Gregory^{1,4}**

5 ¹NCAS, University of Reading, Reading, UK

6 ²Max Planck Institute for Meteorology, Hamburg, Germany

7 ³Department of Atmospheric Science, Colorado State University, Fort Collins, CO, USA

8 ⁴Met Office Hadley Centre, Exeter, UK

9 **Key Points:**

- 10 • Equilibrium warming per CO₂ doubling increases with CO₂ level for 13 of 14 cli-
11 mate models.
12 • Positive feedback temperature dependence explains most of the sensitivity increase.
13 • Nonlinear feedbacks increase the long-term risk of extreme warming under high
14 CO₂ emissions.

Abstract

Equilibrium climate sensitivity - the equilibrium warming per CO₂ doubling - increases with CO₂ concentration for thirteen of fourteen coupled general circulation models for 0.5 to 8 times the preindustrial concentration. In particular, the abrupt4xCO₂ equilibrium warming is more than twice the 2xCO₂ warming. We identify three potential causes: nonlogarithmic forcing, feedback CO₂ dependence, and feedback temperature dependence. Feedback temperature dependence explains at least half of the sensitivity increase, while feedback CO₂ dependence explains a smaller share, and nonlogarithmic forcing decreases sensitivity in as many models as it increases it. Feedback temperature dependence is positive for ten out of fourteen models, primarily due to the longwave clear-sky feedback, while cloud feedbacks drive particularly large sensitivity increases. Feedback temperature dependence increases the risk of extreme or runaway warming, and is estimated to cause six models to warm at least an additional 3K under 8xCO₂.

Plain Language Summary

Increasing CO₂ reduces the rate at which energy leaves Earth, causing a net energy gain at its surface. The resulting warming increases the rate that energy leaves the planet. The planet stops warming once it regains balance. Studies usually assume that doubling atmospheric CO₂ always produces the same eventual global temperature rise (called the “equilibrium climate sensitivity”), whatever the starting CO₂ level. We show, on the contrary, that in nearly all the computer climate models we have examined, the extra warming for each doubling goes up as the CO₂ level increases. In most models, the warmer the climate becomes, the more it has to warm in order to balance a further CO₂ doubling, because warming becomes less effective at rebalancing the flow of energy. This effect increases projections of warming, especially for scenarios of greatest CO₂ increase.

1 Introduction

The *equilibrium climate sensitivity* (ΔT_{2x}) is the equilibrium global-mean surface warming per CO₂ doubling (Hansen et al., 1985; Stocker et al., 2013). ΔT_{2x} is often assumed to be constant (Stocker et al., 2013), allowing the equilibrium warming from different CO₂ increases to be characterized by a single metric, and for time series with various CO₂ changes to be used to estimate ΔT_{2x} . A constant ΔT_{2x} rests on two assumptions: each CO₂ doubling induces the same radiative forcing, and each unit of forcing induces the same equilibrium warming (i.e., that the net radiative feedback is constant). However, for low or high enough CO₂ concentrations, the net radiative feedback becomes positive, causing runaway glaciation (Hoffman et al., 1998) or a runaway greenhouse (Komabayasi, 1967; Ingersoll, 1969) respectively. Given these limits, will ΔT_{2x} remain constant across the range of CO₂ levels expected under future emissions scenarios?

Paleoclimatologists have investigated this question (Heydt et al., 2016; Farnsworth et al., 2019). Studies of the early Cenozoic find an increase in climate sensitivity with CO₂ concentration (Caballero & Huber, 2013; Anagnostou et al., 2016; Shaffer et al., 2016; Farnsworth et al., 2019; Zhu et al., 2019; Anagnostou et al., 2020), while studies of the Pleistocene disagree about whether sensitivity increases (three of four models in Crucifix, 2006; Yoshimori et al., 2009; Friedrich et al., 2016; Köhler et al., 2017; Snyder, 2019), stays the same (Martínez-Botí et al., 2015), or decreases (one of four models in Crucifix, 2006) with CO₂. However, different continental configurations may affect how sensitivity changes with CO₂ (Caballero & Huber, 2013; Wolf et al., 2018; Farnsworth et al., 2019).

While most studies of general circulation models under modern conditions have found that sensitivity increases with CO₂ (Hansen et al., 2005; Bitz et al., 2012; Block & Mauritsen, 2013; Caballero & Huber, 2013; Jonko et al., 2013; Meraner et al., 2013; Gregory

et al., 2015; Rieger et al., 2017; Duan et al., 2019; Rohrschneider et al., 2019), some have found that it decreases (Stouffer & Manabe, 2003; Kutzbach et al., 2013) or remains roughly constant (Colman & McAvaney, 2009). However, these thirteen studies only evaluate ΔT_{2x} for models from five modelling centers. In most cases they use mixed-layer oceans, neglecting changes in ocean dynamics that can affect sensitivity (Kutzbach et al., 2013; Farnsworth et al., 2019).

Recently, two datasets have become available with coupled atmosphere-ocean general circulation model (AOGCM) simulations at multiple constant CO₂ levels initialized under preindustrial conditions (abrupt nx CO₂ simulations, where nx CO₂ refers to the increase relative to preindustrial CO₂ concentration): ten Coupled Model Intercomparison Project Phase 6 (CMIP6) models with abrupt0.5xCO₂ and abrupt2xCO₂ simulations run as part of NonLinMIP (Good et al., 2016) in addition to the standard abrupt4xCO₂ simulations (Eyring et al., 2016), and five models in the LongRunMIP archive (a collection of 1000+ year simulations of coupled AOGCMs; Rugenstein et al., 2019) with abrupt2xCO₂, abrupt4xCO₂, and abrupt8xCO₂ simulations. One model participated in both projects.

In this paper, we show that equilibrium climate sensitivity generally increases with CO₂ level (Section 2); that changes in radiative forcing are not large enough to explain this increase for most models (Section 3); and that the increase is instead caused by positive feedback temperature dependence, with some contribution from feedback CO₂ dependence (Section 4). We compare these three nonlinear terms and their causes (Section 5) and then summarize our findings (Section 6).

2 Equilibrium warming

Let T be the globally-averaged surface temperature, and $\Delta T \equiv T - T_{pi}$ be the warming relative to the preindustrial period. We define $\Delta T_{eq}(C)$ as the equilibrium warming caused by changing the CO₂ concentration from its preindustrial value ($pCO_{2,pi} \approx 280$ ppm) to a new value (pCO_2), where C is the number of CO₂ doublings relative to this preindustrial period,

$$C(pCO_2) \equiv \log_2 \left(\frac{pCO_2}{pCO_{2,pi}} \right) \quad (1)$$

Under preindustrial conditions, $C_{pi} = 0$; in an abrupt2xCO₂ simulation, $C = 1$; and so forth. Table S1 is a glossary of all symbols used in this paper.

One condition for equilibrium is that the net top-of-atmosphere radiative flux N (downwards positive) is zero, on average. If we assume that N depends solely on C and T , then we can express a change in N in an abrupt nx CO₂ simulation as an initial change due to C and a subsequent change due to T :

$$N(C, T) - N(C_{pi}, T_{pi}) = (N(C, T_{pi}) - N(C_{pi}, T_{pi})) + (N(C, T) - N(C, T_{pi})) \quad (2)$$

$$= (N(C, T_{pi}) - N(C_{pi}, T_{pi})) + \int_{T_{pi}}^{T_{pi} + \Delta T} \frac{\partial N(C, T)}{\partial T} dT \quad (3)$$

$$= F(C_{pi}, T_{pi}, C) + \int_{T_{pi}}^{T_{pi} + \Delta T} \lambda(C, T) dT \quad (4)$$

F is the *radiative forcing*, the change in N relative to a given initial condition (C_i, T_i) caused by C doublings of CO₂ while holding surface temperature fixed ($F(C_i, T_i, C) \equiv N(C_i + C, T_i) - N(C_i, T_i)$), and λ is the *radiative feedback*, the dependence of N on T ($\lambda(C, T) \equiv \partial N(C, T) / \partial T$), where the sign convention implies the feedback is typically negative. We can find $\Delta T_{eq}(C)$ by setting $N(C, T) = 0$:

$$F(C_{pi}, T_{pi}, C) = - \int_{T_{pi}}^{T_{pi} + \Delta T_{eq}(C)} \lambda(C, T) dT \quad (5)$$

102 where we assume $N(C_{pi}, T_{pi}) = 0$, since the preindustrial climate was roughly in equi-
 103 librium.

104 Under preindustrial concentrations, the spectral line shape of CO₂ absorption bands
 105 creates a logarithmic dependence of N on changes in pCO_2 , so that the *forcing per CO₂*
 106 *doubling* ($\tilde{F} \equiv \partial N / \partial C$) is often assumed to be constant (Myhre et al., 1998). Our def-
 107 inition of radiative forcing also includes adjustments of the atmosphere, land, and ocean
 108 to CO₂ changes that occur independently of subsequent changes in surface temperature
 109 (e.g., Sherwood et al., 2014; Kamae et al., 2015). This “effective radiative forcing” is also
 110 often assumed to be constant per CO₂ doubling (Forster et al., 2016), as is the radiative
 111 feedback (Hansen et al., 1985; Gregory et al., 2004). Substituting these constant terms
 112 into Eq. 5, we can solve for $\Delta T_{eq}(C)$:

$$\Delta T_{eq}(C) = -\frac{\tilde{F}}{\lambda} C \quad (6)$$

113 Assuming a constant \tilde{F} and λ is equivalent to approximating $N(T, C)$ with the linear
 114 Taylor expansion of N around preindustrial values of C_{pi} and T_{pi} (i.e., $N(C, T) \approx \tilde{F}C +$
 115 $\lambda\Delta T$, where $C = \Delta C$ because $C_{pi} = 0$). The linear approximation of Eq. 6 is ubiqui-
 116 tuous in climate science (e.g., Stocker et al., 2013; Knutti et al., 2017).

117 The linear approximation implies that the *equilibrium climate sensitivity* (ΔT_{2x}),
 118 the equilibrium warming per CO₂ doubling, is simply $-\tilde{F}/\lambda$, which, being a ratio of two
 119 constants, is itself a constant. It should therefore not matter how many CO₂ doublings
 120 are used to estimate it, since $\Delta T_{2x} = \Delta T_{eq}(C_1)/C_1 = \Delta T_{eq}(C_2)/C_2$. Fig. 1a shows
 121 instead that our estimates of $\Delta T_{eq}(C)/C$ increase with CO₂ concentration for thirteen
 122 of fourteen models. Colored bars show estimates made by extrapolating regressions of
 123 years 21 to 150 of N against ΔT to equilibrium ($N = 0$) for abrupt2xCO₂ simula-
 124 tions (Gregory et al., 2004, see also solid gray lines in Fig. S1). In these estimates, N
 125 and ΔT are anomalies: for LongRunMIP, we subtract the model’s control simulation’s
 126 mean value; for CMIP6, we subtract the linear fit of the control simulation after the branch
 127 point for the abruptnxCO₂ simulations. We use only one ensemble member for each sim-
 128 ulation.

129 Estimates of ΔT_{eq} typically increase with simulation length (Rugenstein et al., 2020;
 130 Dai et al., 2020; Dunne et al., 2020). While most CMIP6 simulations are only 150 years
 131 long, some are longer, and the LongRunMIP models are all at least 1000 years long. Black
 132 horizontal lines in Fig. 1a show estimates using years 101 to 750+ (see Table S2 for ex-
 133 act number of years). Here and in the following we use bootstrapping to estimate the
 134 2.5th to 97.5th percentile range of uncertainty (gray and black vertical lines in Fig. 1;
 135 see Text S1). Black bars show multi-model mean values for the two experiments for which
 136 we have simulations of all models.

137 The sensitivity definition in Fig. 1a (i.e., $\Delta T_{2x}(C) \equiv \Delta T_{eq}(C)/C$) is often used
 138 to estimate ΔT_{2x} from abrupt4xCO₂ simulations, which our results suggest would lead
 139 to an average overestimate of at least 0.5K, even neglecting the outlier of FAMOUS. Equiv-
 140 alently, the nonlinearity of N leads to an average increase in equilibrium warming of at
 141 least 1K under 4xCO₂. Sherwood et al. (2020) suggested that using only the first 150
 142 years to estimate ΔT_{eq} of an abrupt4xCO₂ simulation compensates for this overestimate.
 143 For our five models with 1000+ year abrupt2xCO₂ simulations, this compensation does
 144 not hold individually (CNRM-CM6-1’s ΔT_{2x} would be 0.4K too small, FAMOUS’s 1.8K
 145 too large), or on average (an 8% overestimate). If we define sensitivity instead as the equi-
 146 librium warming caused by successive CO₂ doublings ($\Delta T_{2x}(C) \equiv \Delta T_{eq}(C) - \Delta T_{eq}(C-$
 147 $1)$; Jonko et al., 2013), then changes in sensitivity are larger, with increases larger than
 148 1K for seven models (Fig. S2). Alternatively, if we define sensitivity as the warming from
 149 doubling CO₂ relative to preindustrial conditions only ($\Delta T_{2x} \equiv \Delta T_{eq}(1)$; e.g., Knutti
 150 et al., 2017; Ceppi & Gregory, 2017), our results suggest that this metric may have a lim-
 151 ited applicability.

152 The above shows that the equilibrium climate sensitivity is inconstant, and thus
 153 the linear approximation is inaccurate. To understand the increase in sensitivity, we take
 154 the quadratic Taylor expansion of N around (C_{pi}, T_{pi}) :

$$N(C, T) \approx \frac{\partial N}{\partial C} \Big|_{C=C_{pi}, T=T_{pi}} C + \frac{\partial N}{\partial T} \Big|_{C=C_{pi}, T=T_{pi}} \Delta T + \frac{1}{2} \left(\frac{\partial^2 N}{\partial C^2} C^2 + \frac{\partial^2 N}{\partial T^2} (\Delta T)^2 + 2 \frac{\partial^2 N}{\partial C \partial T} C \Delta T \right) \quad (7)$$

155 Substituting these new terms into Eq. 5, we have:

$$(\tilde{F}_{pi} + \frac{1}{2} \partial_C \tilde{F} C) C = -(\lambda_{pi} + \partial_C \lambda C + \frac{1}{2} \partial_T \lambda \Delta T_{eq}) \Delta T_{eq} \quad (8)$$

156 where $\tilde{F}_{pi} \equiv \frac{\partial N}{\partial C} \Big|_{C_{pi}, T_{pi}}$ and $\lambda_{pi} \equiv \frac{\partial N}{\partial T} \Big|_{C_{pi}, T_{pi}}$ are the *preindustrial forcing per CO₂ dou-*
 157 *bling* and *preindustrial feedback* respectively, $\partial_C \tilde{F} \equiv \frac{\partial^2 N}{\partial C^2}$ is the CO₂ dependence of the
 158 forcing per doubling (which we call the *nonlinear forcing*), $\partial_C \lambda \equiv \frac{\partial^2 N}{\partial C \partial T}$ is the *feedback*
 159 *CO₂ dependence*, and $\partial_T \lambda \equiv \frac{\partial^2 N}{\partial T^2}$ is the *feedback temperature dependence*.

160 The three nonlinear terms ($\partial_C \tilde{F}$, $\partial_C \lambda$, and $\partial_T \lambda$) can all cause the equilibrium cli-
 161 mate sensitivity to change with CO₂ concentration. Solving for $\Delta T_{eq}(C)$, we have

$$\Delta T_{eq}(C) = \frac{-(\lambda_{pi} + \partial_C \lambda C) - \sqrt{(\partial_C \lambda^2 - \partial_T \lambda \partial_C \tilde{F}) C^2 + 2(\lambda_{pi} \partial_C \lambda - \tilde{F}_{pi} \partial_T \lambda) C + \lambda_{pi}^2}}{\partial_T \lambda} \quad (9)$$

162 We ignore the other quadratic solution, which gives an unstable equilibrium for C . In
 163 the following sections, we consider the impact of these terms on ΔT_{eq} .

164 3 Radiative forcing

165 Direct forcing depends linearly on C for small C (Myhre et al., 1998, who estimate
 166 $F(C) = 3.71C \text{ Wm}^{-2}$; dashed black line, Fig. 1b). At higher CO₂ levels, new absorp-
 167 tion bands make this dependence superlinear (Byrne & Goldblatt, 2014; Etminan et al.,
 168 2016). Using the left side of Eq. 8, we have

$$F(C_{pi}, T_{pi}, C) = \tilde{F}_{pi} C + \frac{1}{2} \partial_C \tilde{F} C^2 \quad (10)$$

169 Byrne and Goldblatt (2014) used line-by-line radiative calculations and a simple strato-
 170 spheric adjustment model to estimate $\tilde{F}_{pi} = 3.69 \text{ Wm}^{-2}$ and $\partial_C \tilde{F} = 0.375 \text{ Wm}^{-2}$ for
 171 0.7xCO₂ to 36xCO₂, implying an increase in forcing per doubling with CO₂ concentra-
 172 tion (gray bars in Fig. 1b).

173 We estimate forcing per doubling for each simulation (colored bars, Fig. 1b) by re-
 174 gressing the first ten years of N vs. ΔT to $\Delta T = 0$ (dashed black lines in Fig. S1; Gre-
 175 gory et al., 2004). This estimate includes adjustments as well as direct effects. Forcing
 176 per doubling decreases with C about as often as it increases, so that nonlinear forcing
 177 cannot explain the general increase in sensitivity. For CO₂ levels for which we have sim-
 178 ulations for all models (2xCO₂ and 4xCO₂), the multi-model mean forcing per doubling
 179 slightly decreases with C , although this decrease is not statistically significant.

180 Sensitivity increases with CO₂ concentration by a greater factor than forcing per
 181 doubling for most models (Fig. 1c). While all simulations but one have superlinear warm-
 182 ing (i.e., are right of the vertical dashed line), nine simulations have sublinear forcing (i.e.,
 183 are below the horizontal dashed line). Thirteen out of seventeen simulations have a smaller
 184 forcing increase than a warming increase (i.e. fall below the 1-to-1 line), as do the multi-
 185 model means. Moreover, there is little correlation between the nonlinear warming and
 186 forcing factors ($R^2 = 0.05$), even ignoring models with anomalous sensitivity increases
 187 (FAMOUS and CESM2; $R^2 = 0.14$). Forcing does not play a large role in the sensitiv-
 188 ity increase for most models, although it may for individual models (e.g., CESM1.0.4).

Using twenty years instead of ten to estimate F reduces uncertainty (Fig. S3a) but biases estimates of F low, because of an increase in the slope of N vs. ΔT over time (Fig. S3b), and has little effect on our findings in Fig. 1c (see Fig. S3c). Sensitivity also increases by a greater factor than would be implied by Byrne and Goldblatt (2014) (Fig. S3d). Our findings are also the same if we first estimate \tilde{F}_{pi} and $\partial_C \tilde{F}$ for each model by fitting the quadratic function in Eq. 10 (Figs. S4a and S4b): $\partial_C \tilde{F}$ is positive for only half of the models, with multi-model mean values of $\tilde{F}_{pi} = 4.01 \text{ Wm}^{-2}$ and $\partial_C \tilde{F} = 0.017 \text{ Wm}^{-2}$.

4 Radiative feedback

If sensitivity is not proportional to forcing, then Eq. 5 implies the feedback is inconstant. Inconstant feedbacks are commonly associated with the ‘‘pattern effect,’’ in which the slope of N vs. ΔT under constant forcing varies. This slope is the weighted average of the spatial pattern of feedbacks, where the weights are given by the spatial pattern of surface warming, which evolves primarily due to the warming delay in regions of deep ocean heat uptake (e.g., Senior & Mitchell, 2000; Armour et al., 2013; Andrews et al., 2015; Rose et al., 2014; Rugenstein et al., 2016; Zhou et al., 2017; Dong et al., 2019; Bloch-Johnson et al., 2020).

The framework in Section 2 does not account for spatially-varying feedbacks, which make $N(C, T)$ an ill-defined function, in that it can have multiple values: the same globally-averaged T with warmer temperatures in regions with strong negative feedbacks implies a lower N than if the surface temperature was spatially uniform. It is more accurate to define $N(C, \vec{T})$, where $\Delta \vec{T}$ is the spatial temperature pattern (Haugstad et al., 2017). This means that the equilibrium response cannot generally be estimated from the slope of N vs. ΔT , which may evolve differently at different forcing levels simply because the patterns of warming associated with each simulation are different. For example, it is possible for the slope of N vs. ΔT to change due to a pattern effect, but for the overall response to forcing to be linear, so that the equilibrium climate sensitivity is constant (Rohrschneider et al., 2019).

To create a tractable framework, we assume that every globally-averaged surface temperature T is associated with a unique equilibrium pattern, $\vec{T}_{eq}(T)$, which is the pattern when T is in equilibrium (stable or unstable) for some C . We then substitute N with $N_{eq}(C, T) \equiv N(C, \vec{T}_{eq}(T))$ in our above definitions of λ and F . This substitution does not affect our forcing definition, as forcing is typically defined with respect to an equilibrated state, but ensures that any change in the feedback implies a change in the proportionality of $F(C)$ to $\Delta T_{eq}(C)$, and vice versa, as expected from Eq. 5. It also implies that the only way in which the pattern effect affects the equilibrium climate sensitivity is through changes in the equilibrium pattern of warming.

From Eq. 8, we have:

$$\lambda(C, T) = \lambda_{pi} + \partial_C \lambda C + \partial_T \lambda \Delta T \quad (11)$$

where $\lambda_{pi} \equiv \partial N / \partial T|_{pi}$ is the preindustrial feedback, $\partial_C \lambda \equiv \partial \lambda / \partial C = \partial^2 N / \partial C \partial T$ represents the feedback CO_2 dependence, and $\partial_T \lambda \equiv \partial \lambda / \partial T = \partial^2 N / \partial T^2$ represents the feedback temperature dependence (Roe & Armour, 2011; Bloch-Johnson et al., 2015).

Feedback CO_2 dependence quantifies the effect of additional atmospheric CO_2 on radiative feedbacks, such as damping the Planck feedback by making more frequencies optically thick (Seeley & Jeevanjee, 2020). It can also include effects due to forcing adjustments. The pattern effect prevents us from comparing the slope of N vs. ΔT across forcing levels to estimate $\partial_C \lambda$. Instead, we use additional experiments for five coupled AOGCMs, CESM1.2.2, CESM2*, CNRM-CM6-1*, HadGEM2, and HadGEM3-GC31-LL* (starred models are from our main analysis; see Table S3 and Text S2), to estimate

237 $\partial_C \lambda$. Since $\partial \lambda / \partial C \equiv \partial^2 N / \partial C \partial T = \partial \tilde{F} / \partial T$, feedback CO₂ dependence is also the de-
 238 pendence of the forcing per doubling on the reference temperature. We use pairs of ex-
 239 periments initialized at a colder temperature (T_{cold}) and a warmer temperature (T_{warm})
 240 and the same initial CO₂ concentration C_i to estimate forcing from the same amount
 241 of CO₂ doubling C :

$$\partial_C \lambda = \partial_T \tilde{F} \approx \frac{1}{\Delta T} \frac{\Delta F(C_i, T_i, C)}{C} = \frac{F_{warm} - F_{cold}}{(T_{warm} - T_{cold})C} \quad (12)$$

242 where $F_{warm} \equiv F(C_i, T_{warm}, C)$ and $F_{cold} \equiv F(C_i, T_{cold}, C)$.

243 F_{cold} and F_{warm} can be estimated using pairs of abrupt simulations (i.e., an abrupt4xCO₂
 244 simulation to estimate F_{cold} , and a simulation where CO₂ is abruptly lowered from 4xCO₂
 245 to preindustrial values to estimate $-F_{warm}$) or from two pairs of fixed-SST experiments
 246 (Hansen et al., 2005) at two different temperatures and CO₂ concentrations. $\partial_C \lambda$ has
 247 a multi-model mean value of $\partial_C \lambda_{mean} = 0.0256 \text{ Wm}^{-2}\text{K}^{-1}$ and a range of 0.0057 to
 248 0.049 $\text{Wm}^{-2}\text{K}^{-1}$, suggesting that feedback CO₂ dependence is generally positive, increas-
 249 ing sensitivity with CO₂ concentration.

250 To estimate each model’s feedback temperature dependence, we perform a least squares
 251 fit of Eq. 8 using estimates of \tilde{F}_{pi} and $\partial_C \tilde{F}$ from the previous section, as well as model-
 252 specific estimates of $\partial_C \lambda$ when available, or otherwise $\partial_C \lambda_{mean}$. We perform this fit us-
 253 ing pairs of C and ΔT_{eq} for each simulation, including the pair $C = 0$ and $\Delta T_{eq} = 0$
 254 for the control simulation, giving estimates of λ_{pi} and $\partial_T \lambda$ (colored dots, Fig. 2). We
 255 find that ten of the fourteen models have positive feedback temperature dependence, with
 256 a multi-model mean value of $\partial_T \lambda_{mean} = 0.029 \text{ Wm}^{-2}\text{K}^{-2}$ and a range of -0.14 to 0.109
 257 $\text{Wm}^{-2}\text{K}^{-2}$.

258 With positive feedback temperature dependence, warming increases the feedback,
 259 leading to further warming, and so on. Under sufficient forcing, runaway warming oc-
 260 curs (Zaliapin & Ghil, 2010; Bloch-Johnson et al., 2015), specifically when Eq. 9 has no
 261 real solution ($\partial_T \lambda > (\lambda_{pi} + \partial_C \lambda C)^2 / (\partial_C \tilde{F} C^2 + 2\tilde{F}_{pi} C)$), as shown by the light gray re-
 262 gion for 8xCO₂ and dark gray region for 4xCO₂ (assuming that radiative forcing follows
 263 Byrne and Goldblatt (2014) and $\partial_C \lambda = \partial_C \lambda_{mean}$). FAMOUS falls in the latter region,
 264 and its abrupt4xCO₂ simulation does appear to lose its negative feedback (Fig. S1); four
 265 models lie in the 8xCO₂ runaway region. Climates in the gray regions do not actually
 266 warm infinitely, but simply warm sufficiently that the quadratic approximation breaks.
 267 Higher-order terms determine the temperature at which stability is regained, or if sta-
 268 bility is lost in the first place. Models close to these runaway regions experience a sensi-
 269 tivity increase at the associated forcing level: the six models with black outlines ex-
 270 perience an estimated increase of equilibrium warming under 8xCO₂ of at least 3K, given
 271 each model’s forcing and $\partial_C \lambda$ estimates.

272 High estimated sensitivity ($\Delta T_{4x} / 2 > 4.5K$) has been found in twenty CMIP6
 273 models (Table S4). Of the six models with $\Delta T_{4x} / 2 > 4.5K$ that appear in our study
 274 (i.e., models right of the dotted line in Fig. 2), four have $\Delta T_{2x} < 4.5K$ (i.e., are left
 275 of the dashed line). These models reconcile the moderate ΔT_{2x} implied by observations,
 276 paleoclimate, and processed-based analysis (Sherwood et al., 2020) with the sensitivity
 277 increases seen in paleoclimate studies of the warm Cenozoic (Caballero & Huber, 2013;
 278 Pierrehumbert, 2013; Anagnostou et al., 2016; Shaffer et al., 2016; Farnsworth et al., 2019).

279 To test the assumptions behind Fig. 2, we recalculate it with default values of $\partial_C \lambda =$
 280 0 and 0.05 $\text{Wm}^{-2}\text{K}^{-1}$ (Fig. S5a and S5b, respectively). This shifts the estimates of $\partial_T \lambda$
 281 in the opposite direction as $\partial_C \lambda$, but also shifts the thresholds in the same manner, so
 282 that qualitatively the results are unchanged. Estimating forcing using years 1-20 instead
 283 of 1-10 has little effect (Fig. S5c), nor does using the direct estimate of $F(C)$ instead of
 284 $(\tilde{F}_{pi} + \frac{1}{2} \partial_C \tilde{F} C)C$ on the left side of Eq. 8 (Fig. S5d). Fig. S5e shows how $\partial_T \lambda$ evolves
 285 as more years are used to estimate the equilibrium warming. While more years do not

286 greatly affect the results relative to each other, using years 101-1000 instead of 21-150
 287 increases the magnitude of $\partial_T \lambda$ (excepting FAMOUS, which appears to be in a state of
 288 runaway). Since feedback temperature dependence should continue to affect the slope
 289 of N vs. ΔT beyond year 150 (Rugenstein et al., 2020), our estimates of CMIP6 mod-
 290 els' $|\partial_T \lambda|$ and sensitivity changes may both be biased low.

291 5 Causes of sensitivity increases

292 Fig. 3a compares the contribution of the three nonlinear terms to each model's change
 293 in equilibrium climate sensitivity, $\Delta\Delta T_{2x} \equiv \Delta T_{4x}/2 - \Delta T_{2x}$. Using Eq. 9 to express
 294 equilibrium warming as a function of the quadratic approximation coefficients, $\Delta T_{eq}(C; \tilde{F}_{pi}, \lambda_{pi}, \partial_C \tilde{F}, \partial_C \lambda, \partial_T \lambda)$,
 295 we define:

$$\Delta\Delta T_{2x, \partial_C \tilde{F}} \equiv \Delta T_{eq}(2; \tilde{F}_{pi}, \lambda_{pi}, \partial_C \tilde{F}, 0, 0)/2 - \Delta T_{eq}(1; \tilde{F}_{pi}, \lambda_{pi}, \partial_C \tilde{F}, 0, 0) \quad (13)$$

$$\Delta\Delta T_{2x, \partial_C \lambda} \equiv \Delta T_{eq}(2; \tilde{F}_{pi}, \lambda_{pi}, 0, \partial_C \lambda, 0)/2 - \Delta T_{eq}(1; \tilde{F}_{pi}, \lambda_{pi}, 0, \partial_C \lambda, 0) \quad (14)$$

$$\Delta\Delta T_{2x, \partial_T \lambda} \equiv \Delta T_{eq}(2; \tilde{F}_{pi}, \lambda_{pi}, 0, 0, \partial_T \lambda)/2 - \Delta T_{eq}(1; \tilde{F}_{pi}, \lambda_{pi}, 0, 0, \partial_T \lambda) \quad (15)$$

296 Feedback temperature dependence is the dominant term for the three models with the
 297 largest sensitivity increases, accounts for 69% of the average increase, and contributes
 298 the largest term to the median increase (where FAMOUS is excluded from the averages,
 299 as the quadratic model suggests it experiences runaway warming under 4xCO₂). Feed-
 300 back CO₂ dependence contributes a small, positive increase in sensitivity, while nonlin-
 301 ear forcing decreases sensitivity about as much and as often as it increases it.

302 To better understand these sensitivity increases, we estimate the flux components
 303 of the preindustrial feedback and feedback temperature dependence (Fig. 3b-d; see Fig.
 304 S6 for all components and uncertainties) by substituting individual top-of-atmosphere
 305 fluxes for N in the above derivations (see Text S3). We consider longwave vs. shortwave
 306 and noncloud vs. cloud components. For longwave fluxes, noncloud vs. cloud compo-
 307 nents are estimated using clear-sky fluxes and cloud radiative effect. For shortwave fluxes,
 308 to avoid cloud masking (Soden et al., 2004) we instead use approximate partial radiative
 309 perturbation (APRP; Taylor et al., 2007) for models with sufficient data available,
 310 including most CMIP6 models. For all other models we use clear-sky fluxes and cloud
 311 radiative effect as with the longwave.

312 The longwave noncloud feedback typically has positive temperature dependence
 313 (colored circles, Fig. 3b) due to an increasing water vapor feedback (Crucifix, 2006; Col-
 314 man & McAvaney, 2009; Meraner et al., 2013). While some studies found that this in-
 315 crease is balanced by a strengthening negative lapse rate feedback (Boer et al., 2005; Col-
 316 man & McAvaney, 2009; Yoshimori et al., 2009; Caballero & Huber, 2013), in recent stud-
 317 ies the water vapor feedback dominates (Block & Mauritsen, 2013; Jonko et al., 2013;
 318 Meraner et al., 2013; Rieger et al., 2017), and Meraner et al. (2013) found a positive $\partial_T \lambda_{LW noncloud}$
 319 for most CMIP5 models. Our findings contradict recent papers that find a constant long-
 320 wave clear-sky feedback (Koll & Cronin, 2018; Zhang et al., 2020), though we agree that
 321 the value of the preindustrial feedback is likely close to -2 Wm⁻²K⁻¹.

322 The shortwave noncloud feedback (colored circles, Fig. 3c) is the sum of a surface
 323 term (Fig. S6e) and an atmosphere term (Fig. S6f). The former represents a positive
 324 ice albedo feedback, which typically saturates, giving a negative temperature dependence
 325 (Colman & McAvaney, 2009; Block & Mauritsen, 2013; Jonko et al., 2013; Meraner et
 326 al., 2013; Rieger et al., 2017; Duan et al., 2019). The noncloud atmosphere term repre-
 327 sents a positive water vapor feedback, which typically has a positive temperature depen-
 328 dence. Their sum has a positive preindustrial feedback with negligible temperature depen-
 329 dence (Fig. 3c). The SW noncloud outliers are models for which clear-sky fluxes were
 330 used instead of APRP (circles with black dots, Fig. 3c). Comparison of clear-sky vs. APRP
 331 estimates of the SW noncloud component suggests that cloud masking biases generally
 332 increases the uncertainty of the SW noncloud component (Fig. S6c vs. S6g).

333 While the cloud feedback has multi-model mean values close to zero, it has more
 334 intermodel spread than the other two components (Fig. 3d) and has positive temper-
 335 ature dependence for most models. For CESM2, this occurs because its negative mixed-
 336 phase cloud feedback saturates (Tan et al., 2016; Frey & Kay, 2018; Bjordal et al., 2020).
 337 The spread in cloud feedback explains the range of nonlinearity in Fig. 3a. The aver-
 338 age longwave noncloud feedback on its own (gray circle in Fig. 3b) would experience too
 339 little warming for its temperature dependence to matter (i.e., $\Delta\Delta T_{2x} = \Delta T_{4x}/2 - \Delta T_{2x} \approx$
 340 0.17K assuming forcing from Byrne and Goldblatt (2014) and average $\partial_C\lambda$). Adding the
 341 shortwave noncloud feedback does not change the temperature dependence, but makes
 342 the preindustrial feedback more positive (gray triangle in Fig. 3b), causing more warm-
 343 ing, increasing the nonlinearity (i.e., $\Delta\Delta T_{2x} \approx 0.33\text{K}$). Adding the average cloud feed-
 344 back causes little change (gray square in Fig. 3b). For individual models, cloud feedbacks
 345 can move the climate into nonlinear regions, either by increasing the preindustrial feed-
 346 back (CanESM5), or by increasing the feedback temperature dependence (CESM2 and
 347 FAMOUS). On the other hand, GISS-E2-2-G’s cloud feedback temperature dependence
 348 is anomalously negative, and therefore it is the only model for which sensitivity decreases
 349 with CO_2 concentration.

350 We briefly discuss the flux components of the other two nonlinear terms (Fig. S7).
 351 The LW clear-sky term of the nonlinear forcing is negative for eleven of fourteen mod-
 352 els (Fig. S7a). Since the direct LW clear-sky forcing depends superlinearly on CO_2 dou-
 353 bling (Byrne & Goldblatt, 2014), this negative term is due either to oversimplifications
 354 in the model’s radiative scheme, or to adjustments. The other components vary in sign,
 355 with the largest source of intermodel spread coming from the cloud components. Since
 356 APRP accounts for cloud masking, the SW cloud spread must also be due to forcing ad-
 357 justments. Adjustments thus play a first-order role in determining nonlinear forcing. The
 358 LW clear-sky component of feedback CO_2 dependence is positive for all five models (Fig.
 359 S7b), likely due to a blocked Planck feedback. SW cloud contributes the largest source
 360 of intermodel spread, so that forcing adjustments also play a first-order role in this non-
 361 linearity.

362 6 Conclusions

363 Equilibrium climate sensitivity increases with CO_2 concentration for thirteen of four-
 364 teen models, contradicting the linear approximation of global energy balance, which as-
 365 sumes a constant forcing per CO_2 doubling and a constant radiative feedback. On av-
 366 erage, climate models experience at least a degree of additional equilibrium warming un-
 367 der $4\times\text{CO}_2$ due to this sensitivity increase. Using a quadratic approximation allows us
 368 to capture the sensitivity increase using three second-order terms: nonlinear forcing, feed-
 369 back CO_2 dependence, and feedback temperature dependence.

370 Feedback temperature dependence explains 69% of the sensitivity increase, and ex-
 371 plains more of the median increase than any other term. Most importantly, it explains
 372 the particularly large increase seen in a handful of models, as positive feedback temper-
 373 ature dependence can cause runaway increases in sensitivity. Four models are predicted
 374 to experience runaway warming under CO_2 concentrations eight times larger than the
 375 preindustrial, and six models are projected to experience at least three additional de-
 376 grees of equilibrium warming under this concentration. Feedback temperature depen-
 377 dence plays a key role in determining the risk of extreme warming in the coming cen-
 378 turies.

379 Ten of fourteen models have positive feedback temperature dependence, primar-
 380 ily due to the longwave clear-sky feedback. Models with large sensitivity increases have
 381 cloud feedbacks with either anomalously positive temperature dependence or anomalously
 382 positive preindustrial values. Feedback CO_2 dependence plays a smaller role, but results
 383 from five models suggests that it is likely positive, increasing sensitivity, primarily due

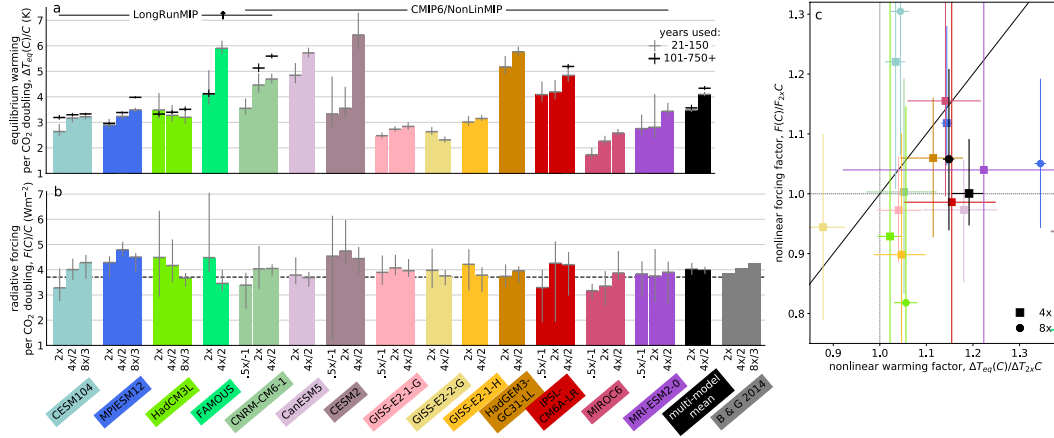


Figure 1. a. Equilibrium warming per CO₂ doubling ($\Delta T_{eq}(C)/C$) for abrupt-2^Cx simulations estimated using years 21 to 150 (colored bars and gray horizontal lines) and years 101 to n (where n is at least 750 years and given in Table S2; black horizontal lines). Vertical lines in panels a and b and all lines in panel c give the 2.5th to 97.5th percentile range of uncertainty (see Text S1). FAMOUS abrupt4xCO₂ is an outlier, with $\Delta T_{4x}/2 = 7.6K$ when 1000 years are used. b. Radiative forcing per CO₂ doubling ($F(C)/C$) for abrupt-2^Cx simulations estimated using years 1 to 10 (colored bars and gray horizontal lines). The dashed black line shows the Myhre et al. (1998) assumption of linear $F(C)$, while the gray bars give the analytic formula from Byrne and Goldblatt (2014). c. Colored squares (octagons) show the factor by which equilibrium warming and forcing for an abrupt4xCO₂ (abrupt8xCO₂) simulation exceeds the linear extrapolation of its model’s abrupt2xCO₂ values. Colors are the same as panels a and b. FAMOUS and CESM2 4x have nonlinear warming factors greater than 1.8.

384 to its longwave clear-sky component. The forcing per CO₂ doubling decreases with CO₂
 385 concentration for as many models as it increases. Nonlinear forcing contributes less to
 386 the sensitivity increase than either other term, although it can be important for individ-
 387 ual models. Forcing adjustments play a first-order role in determining the nonlinear forc-
 388 ing.

389 The substantial uncertainties in some of our findings could be greatly decreased
 390 with additional simulations. Longer simulations give better estimates of equilibrium warm-
 391 ing (Rugenstein et al., 2020; Dai et al., 2020; Dunne et al., 2020); fixed-SST experiments
 392 give better radiative forcing estimates (Forster et al., 2016; Pincus et al., 2016); and sim-
 393 ulations at multiple CO₂ levels allow for an assessment of nonlinearities (Good et al.,
 394 2016). Simulations that behave in surprising or anomalous ways may be exhibiting non-
 395 linear dynamics, and should not be neglected (Valdes, 2011). Even if a loss of stability
 396 causes models to warm outside the range for which they were calibrated, the increase
 397 in sensitivity may still be physical. Exploring and documenting the nonlinear frontiers
 398 of warming in climate models is essential to assessing the risk of extreme warming for
 399 the real world.

400 **Acknowledgments**

401 We thank Tim Andrews for making the HadGEM3-GC3.1-LL abrupt-2xCO₂ simulation
 402 available at <https://github.com/timothyandrews/abrupt-2xCO2>. CMIP6 data is at
 403 <https://pcmdi.llnl.gov/CMIP6/>. LongRunMIP data access is at <http://www.longrunmip>

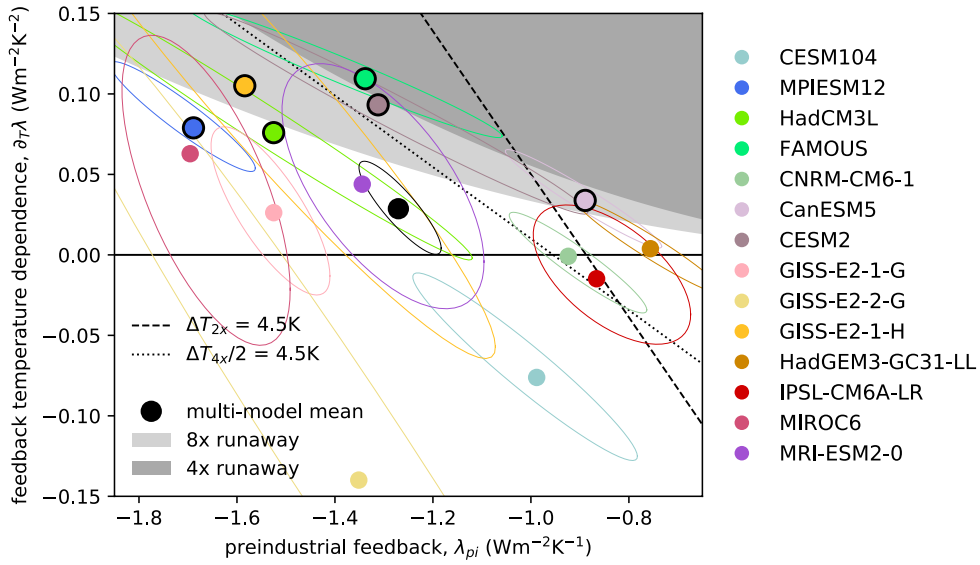


Figure 2. Preindustrial feedback vs. feedback temperature dependence (colored dots; colored ellipsoids give the 75th percentile of uncertainty). Values in the dark (light) gray region imply runaway warming under 4xCO₂ (8xCO₂) and values above the dashed (dotted) black line have a sensitivity estimated from abrupt2xCO₂ (abrupt4xCO₂) above 4.5K. All thresholds are calculated assuming forcing from Byrne and Goldblatt (2014) and model-mean feedback CO₂ dependence. Colored dots with black outlines experience an additional 3K of equilibrium warming under 8xCO₂ given our estimate of that model’s forcing and $\partial_C \lambda$.

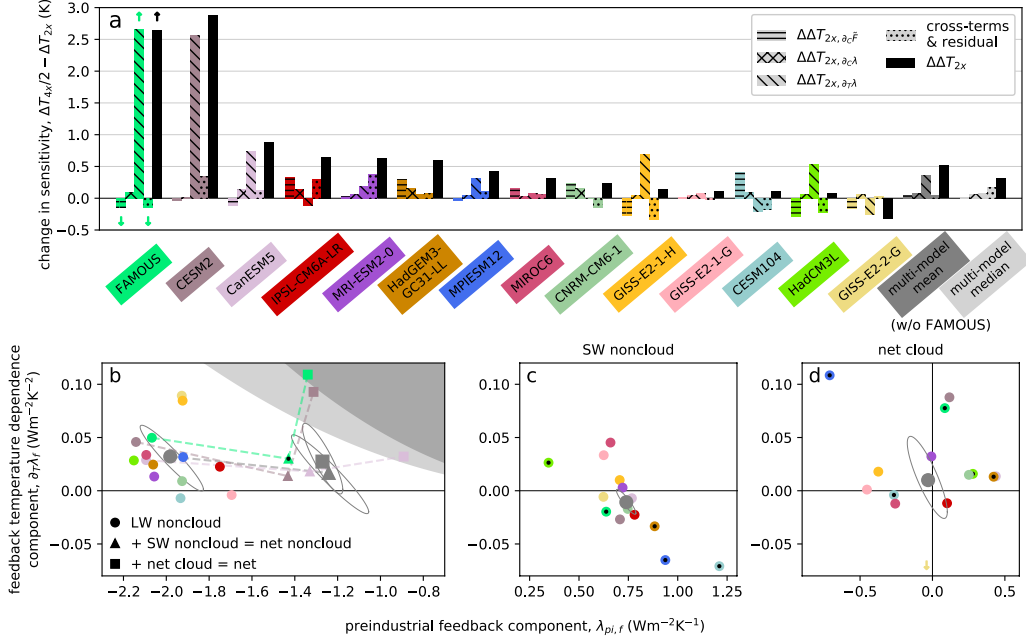


Figure 3. a. Contributions to the change in sensitivity from $2x\text{CO}_2$ to $4x\text{CO}_2$ (black bars) from nonlinear forcing ($\partial_C \tilde{F}$, horizontally-hatched bars), feedback CO_2 dependence ($\partial_C \lambda$, crossed-hatched bars), and feedback temperature dependence ($\partial_T \lambda$, diagonally-hatched bars). Dotted bars represent cross-terms, higher-order nonlinearities, and errors in our estimates. FAMOUS is not included in the mean and median as the quadratic model suggests it is in a state of runaway under $4x\text{CO}_2$.

b., c., and d. Colored circles give estimates of the longwave noncloud, shortwave noncloud, and net cloud components respectively of the preindustrial feedback and feedback temperature dependence. Models with dotted circles use clear-sky fluxes instead of approximate partial radiative perturbation to partition the shortwave flux into noncloud and cloud components. Colors are given by the model names in panel a. Gray circles give the multi-model mean and gray ellipsoids give the estimated 75th percentile of uncertainty. The shaded regions in panel b are as in Fig. 2. Triangles in panel b show the result of adding the shortwave noncloud component to longwave noncloud components. Squares show the result for additionally adding the net cloud component.

404 .org/. This project has received funding from the European Research Council (ERC)
405 under the European Union’s Horizon 2020 research and innovation programme (grant
406 agreement No. 786427, project “Couplet” and grant agreement No. 820829, project “CON-
407 STRAIN”).

References

- 408
- 409 Anagnostou, E., John, E. H., Babila, T. L., Sexton, P. F., Ridgwell, A., Lunt, D. J.,
 410 ... Foster, G. L. (2020, September). Proxy evidence for state-dependence
 411 of climate sensitivity in the Eocene greenhouse. *Nature Communications*,
 412 11(1), 4436. Retrieved 2020-09-11, from <https://www.nature.com/articles/s41467-020-17887-x> (Number: 1 Publisher: Nature Publishing Group) doi:
 413 10.1038/s41467-020-17887-x
 414
- 415 Anagnostou, E., John, E. H., Edgar, K. M., Foster, G. L., Ridgwell, A., Inglis,
 416 G. N., ... Pearson, P. N. (2016). Changing atmospheric CO₂ concentration
 417 was the primary driver of early Cenozoic climate. *Nature*, 533(7603), 380–384.
 418 Retrieved 2019-12-21, from <https://www.nature.com/articles/nature17423>
 419 doi: 10.1038/nature17423
- 420 Andrews, T., Gregory, J. M., & Webb, M. J. (2015). The Dependence of Ra-
 421 diative Forcing and Feedback on Evolving Patterns of Surface Temperature
 422 Change in Climate Models. *Journal of Climate*, 28(4), 1630–1648. Retrieved
 423 2019-11-27, from [https://journals.ametsoc.org/doi/full/10.1175/](https://journals.ametsoc.org/doi/full/10.1175/JCLI-D-14-00545.1)
 424 [JCLI-D-14-00545.1](https://journals.ametsoc.org/doi/full/10.1175/JCLI-D-14-00545.1) doi: 10.1175/JCLI-D-14-00545.1
- 425 Armour, K. C., Bitz, C. M., & Roe, G. H. (2013). Time-Varying Climate Sen-
 426 sitivity from Regional Feedbacks. *Journal of Climate*, 26(13), 4518–4534.
 427 Retrieved 2018-05-12, from [https://journals.ametsoc.org/doi/10.1175/](https://journals.ametsoc.org/doi/10.1175/JCLI-D-12-00544.1)
 428 [JCLI-D-12-00544.1](https://journals.ametsoc.org/doi/10.1175/JCLI-D-12-00544.1) doi: 10.1175/JCLI-D-12-00544.1
- 429 Bitz, C. M., Shell, K. M., Gent, P. R., Bailey, D. A., Danabasoglu, G., Armour,
 430 K. C., ... Kiehl, J. T. (2012). Climate Sensitivity of the Community Climate
 431 System Model, Version 4. *Journal of Climate*, 25(9), 3053–3070. Retrieved
 432 2019-11-27, from [https://journals.ametsoc.org/doi/full/10.1175/](https://journals.ametsoc.org/doi/full/10.1175/JCLI-D-11-00290.1)
 433 [JCLI-D-11-00290.1](https://journals.ametsoc.org/doi/full/10.1175/JCLI-D-11-00290.1) doi: 10.1175/JCLI-D-11-00290.1
- 434 Bjordal, J., Storelvmo, T., Alterskjær, K., & Carlsen, T. (2020, November). Equi-
 435 librium climate sensitivity above 5 C plausible due to state-dependent cloud
 436 feedback. *Nature Geoscience*, 13(11), 718–721. Retrieved 2020-11-20, from
 437 <https://www.nature.com/articles/s41561-020-00649-1> (Number: 11
 438 Publisher: Nature Publishing Group) doi: 10.1038/s41561-020-00649-1
- 439 Bloch-Johnson, J., Pierrehumbert, R. T., & Abbot, D. S. (2015). Feedback tem-
 440 perature dependence determines the risk of high warming. *Geophysical Re-*
 441 *search Letters*, 42(12), 4973–4980. Retrieved 2019-11-27, from [https://](https://agupubs.onlinelibrary.wiley.com/doi/abs/10.1002/2015GL064240)
 442 agupubs.onlinelibrary.wiley.com/doi/abs/10.1002/2015GL064240 doi:
 443 10.1002/2015GL064240
- 444 Bloch-Johnson, J., Rugenstein, M., & Abbot, D. S. (2020). Spatial Radiative Feed-
 445 backs from Internal Variability Using Multiple Regression. *Journal of Climate*,
 446 33(10), 4121–4140. Retrieved 2020-04-22, from [https://journals.ametsoc](https://journals.ametsoc.org/doi/full/10.1175/JCLI-D-19-0396.1)
 447 [.org/doi/full/10.1175/JCLI-D-19-0396.1](https://journals.ametsoc.org/doi/full/10.1175/JCLI-D-19-0396.1) (Publisher: American Meteor-
 448 ological Society) doi: 10.1175/JCLI-D-19-0396.1
- 449 Block, K., & Mauritsen, T. (2013). Forcing and feedback in the MPI-ESM-
 450 LR coupled model under abruptly quadrupled CO₂. *Journal of Advances*
 451 *in Modeling Earth Systems*, 5(4), 676–691. Retrieved 2019-11-27, from
 452 <https://agupubs.onlinelibrary.wiley.com/doi/abs/10.1002/jame.20041>
 453 doi: 10.1002/jame.20041
- 454 Boer, G. J., Hamilton, K., & Zhu, W. (2005). Climate sensitivity and climate change
 455 under strong forcing. *Climate Dynamics*, 24(7), 685–700. Retrieved 2018-
 456 10-31, from <https://doi.org/10.1007/s00382-004-0500-3> doi: 10.1007/
 457 s00382-004-0500-3
- 458 Byrne, B., & Goldblatt, C. (2014). Radiative forcing at high concentrations of
 459 well-mixed greenhouse gases. *Geophysical Research Letters*, 41(1), 152–160.
 460 Retrieved 2019-11-27, from [https://agupubs.onlinelibrary.wiley.com/](https://agupubs.onlinelibrary.wiley.com/doi/abs/10.1002/2013GL058456)
 461 [doi/abs/10.1002/2013GL058456](https://agupubs.onlinelibrary.wiley.com/doi/abs/10.1002/2013GL058456) doi: 10.1002/2013GL058456
- 462 Caballero, R., & Huber, M. (2013). State-dependent climate sensitivity in past

- 463 warm climates and its implications for future climate projections. *Pro-*
 464 *ceedings of the National Academy of Sciences*, 110(35), 14162–14167. Re-
 465 trieved 2018-06-28, from <http://www.pnas.org/content/110/35/14162> doi:
 466 10.1073/pnas.1303365110
- 467 Ceppi, P., & Gregory, J. M. (2017, December). Relationship of tropospheric stabil-
 468 ity to climate sensitivity and Earths observed radiation budget. *Proceedings of*
 469 *the National Academy of Sciences*, 114(50), 13126–13131. Retrieved 2018-06-
 470 28, from <http://www.pnas.org/content/114/50/13126> doi: 10.1073/pnas
 471 .1714308114
- 472 Colman, R., & McAvaney, B. (2009). Climate feedbacks under a very broad
 473 range of forcing. *Geophysical Research Letters*, 36(1). Retrieved 2019-11-
 474 27, from [https://agupubs.onlinelibrary.wiley.com/doi/abs/10.1029/
 475 2008GL036268](https://agupubs.onlinelibrary.wiley.com/doi/abs/10.1029/2008GL036268) doi: 10.1029/2008GL036268
- 476 Crucifix, M. (2006). Does the Last Glacial Maximum constrain climate sensitivity?
 477 *Geophysical Research Letters*, 33(18). Retrieved 2019-12-20, from [https://
 478 agupubs.onlinelibrary.wiley.com/doi/abs/10.1029/2006GL027137](https://agupubs.onlinelibrary.wiley.com/doi/abs/10.1029/2006GL027137) doi:
 479 10.1029/2006GL027137
- 480 Dai, A., Huang, D., Rose, B. E. J., Zhu, J., & Tian, X. (2020, April). Improved
 481 methods for estimating equilibrium climate sensitivity from transient warm-
 482 ing simulations. *Climate Dynamics*. Retrieved 2020-04-23, from [https://
 483 doi.org/10.1007/s00382-020-05242-1](https://doi.org/10.1007/s00382-020-05242-1) doi: 10.1007/s00382-020-05242-1
- 484 Dong, Y., Proistosescu, C., Armour, K. C., Battisti, D. S., Dong, Y., Proistosescu,
 485 C., ... Battisti, D. S. (2019). Attributing Historical and Future Evolution of
 486 Radiative Feedbacks to Regional Warming Patterns using a Greens Function
 487 Approach: The Preeminence of the Western Pacific. *Journal of Climate*. Re-
 488 trieved 2019-09-28, from [https://journals.ametsoc.org/doi/abs/10.1175/
 489 JCLI-D-18-0843.1](https://journals.ametsoc.org/doi/abs/10.1175/JCLI-D-18-0843.1) doi: 10.1175/JCLI-D-18-0843.1
- 490 Duan, L., Cao, L., & Caldeira, K. (2019). Estimating Contributions of Sea Ice
 491 and Land Snow to Climate Feedback. *Journal of Geophysical Research:
 492 Atmospheres*, 124(1), 199–208. Retrieved 2019-12-21, from [https://
 493 agupubs.onlinelibrary.wiley.com/doi/abs/10.1029/2018JD029093](https://agupubs.onlinelibrary.wiley.com/doi/abs/10.1029/2018JD029093) doi:
 494 10.1029/2018JD029093
- 495 Dunne, J. P., Winton, M., Bacmeister, J., Danabasoglu, G., Gettelman,
 496 A., Golaz, J.-C., ... Wolfe, J. D. (2020). Comparison of equi-
 497 librium climate sensitivity estimates from slab ocean, 150-year,
 498 and longer simulations. *Geophysical Research Letters*, n/a(n/a),
 499 e2020GL088852. Retrieved 2020-07-30, from [https://agupubs
 500 .onlinelibrary.wiley.com/doi/abs/10.1029/2020GL088852](https://agupubs.onlinelibrary.wiley.com/doi/abs/10.1029/2020GL088852) (eprint:
 501 <https://agupubs.onlinelibrary.wiley.com/doi/pdf/10.1029/2020GL088852>) doi:
 502 10.1029/2020GL088852
- 503 Efron, B. (1979). Bootstrap Methods: Another Look at the Jackknife. *The Annals*
 504 *of Statistics*, 7(1), 1–26. Retrieved 2020-04-23, from [https://www.jstor.org/
 505 stable/2958830](https://www.jstor.org/stable/2958830) (Publisher: Institute of Mathematical Statistics)
- 506 Etminan, M., Myhre, G., Highwood, E. J., & Shine, K. P. (2016). Radiative forc-
 507 ing of carbon dioxide, methane, and nitrous oxide: A significant revision of
 508 the methane radiative forcing. *Geophysical Research Letters*, 43(24), 12,614–
 509 12,623. Retrieved 2019-11-27, from [https://agupubs.onlinelibrary.wiley
 510 .com/doi/abs/10.1002/2016GL071930](https://agupubs.onlinelibrary.wiley.com/doi/abs/10.1002/2016GL071930) doi: 10.1002/2016GL071930
- 511 Eyring, V., Bony, S., Meehl, G. A., Senior, C. A., Stevens, B., Stouffer, R. J., &
 512 Taylor, K. E. (2016). Overview of the Coupled Model Intercomparison
 513 Project Phase 6 (CMIP6) experimental design and organization. *Geosci-
 514 entific Model Development*, 9(5), 1937–1958. Retrieved 2020-01-10, from
 515 <https://www.geosci-model-dev.net/9/1937/2016/gmd-9-1937-2016.html>
 516 doi: <https://doi.org/10.5194/gmd-9-1937-2016>
- 517 Farnsworth, A., Lunt, D. J., O'Brien, C. L., Foster, G. L., Inglis, G. N., Markwick,

- 518 P., ... Robinson, S. A. (2019). Climate Sensitivity on Geological Timescales
 519 Controlled by Nonlinear Feedbacks and Ocean Circulation. *Geophysical Re-*
 520 *search Letters*, *46*(16), 9880–9889. Retrieved 2019-11-27, from [https://](https://agupubs.onlinelibrary.wiley.com/doi/abs/10.1029/2019GL083574)
 521 agupubs.onlinelibrary.wiley.com/doi/abs/10.1029/2019GL083574 doi:
 522 10.1029/2019GL083574
- 523 Forster, P. M., Richardson, T., Maycock, A. C., Smith, C. J., Samset, B. H., Myhre,
 524 G., ... Schulz, M. (2016). Recommendations for diagnosing effective radiative
 525 forcing from climate models for CMIP6. *Journal of Geophysical Research:*
 526 *Atmospheres*, *121*(20), 12,460–12,475. Retrieved 2019-12-24, from [https://](https://agupubs.onlinelibrary.wiley.com/doi/abs/10.1002/2016JD025320)
 527 agupubs.onlinelibrary.wiley.com/doi/abs/10.1002/2016JD025320 doi:
 528 10.1002/2016JD025320
- 529 Frey, W. R., & Kay, J. E. (2018, April). The influence of extratropical cloud
 530 phase and amount feedbacks on climate sensitivity. *Climate Dynamics*,
 531 *50*(7), 3097–3116. Retrieved 2020-11-23, from [https://doi.org/10.1007/](https://doi.org/10.1007/s00382-017-3796-5)
 532 [s00382-017-3796-5](https://doi.org/10.1007/s00382-017-3796-5) doi: 10.1007/s00382-017-3796-5
- 533 Friedrich, T., Timmermann, A., Tigchelaar, M., Timm, O. E., & Ganopolski, A.
 534 (2016, November). Nonlinear climate sensitivity and its implications for future
 535 greenhouse warming. *Science Advances*, *2*(11), e1501923. Retrieved 2019-12-
 536 20, from <https://advances.sciencemag.org/content/2/11/e1501923> doi:
 537 10.1126/sciadv.1501923
- 538 Good, P., Andrews, T., Chadwick, R., Dufresne, J.-L., Gregory, J. M., Lowe, J. A.,
 539 ... Shiogama, H. (2016). nonlinMIP contribution to CMIP6: model inter-
 540 comparison project for non-linear mechanisms: physical basis, experimental
 541 design and analysis principles (v1.0). *Geoscientific Model Development*, *9*(11),
 542 4019–4028. Retrieved 2019-12-19, from [https://www.geosci-model-dev.net/](https://www.geosci-model-dev.net/9/4019/2016/gmd-9-4019-2016-discussion.html)
 543 [9/4019/2016/gmd-9-4019-2016-discussion.html](https://www.geosci-model-dev.net/9/4019/2016/gmd-9-4019-2016-discussion.html) doi: [https://doi.org/](https://doi.org/10.5194/gmd-9-4019-2016)
 544 [10.5194/gmd-9-4019-2016](https://doi.org/10.5194/gmd-9-4019-2016)
- 545 Gregory, J. M., Andrews, T., & Good, P. (2015, November). The inconstancy
 546 of the transient climate response parameter under increasing CO₂. *Philoso-*
 547 *sophical Transactions of the Royal Society A: Mathematical, Physical and*
 548 *Engineering Sciences*, *373*(2054), 20140417. Retrieved 2020-02-27, from
 549 <https://royalsocietypublishing.org/doi/full/10.1098/rsta.2014.0417>
 550 doi: 10.1098/rsta.2014.0417
- 551 Gregory, J. M., Ingram, W. J., Palmer, M. A., Jones, G. S., Stott, P. A., Thorpe,
 552 R. B., ... Williams, K. D. (2004). A new method for diagnosing radiative
 553 forcing and climate sensitivity. *Geophysical Research Letters*, *31*(3), L03205.
 554 Retrieved 2018-01-19, from [http://onlinelibrary.wiley.com/doi/10.1029/](http://onlinelibrary.wiley.com/doi/10.1029/2003GL018747/abstract)
 555 [2003GL018747/abstract](http://onlinelibrary.wiley.com/doi/10.1029/2003GL018747/abstract) doi: 10.1029/2003GL018747
- 556 Hansen, J., Russell, G., Lacis, A., Fung, I., Rind, D., & Stone, P. (1985). Cli-
 557 mate Response Times: Dependence on Climate Sensitivity and Ocean
 558 Mixing. *Science*, *229*(4716), 857–859. Retrieved 2018-05-15, from
 559 <http://science.sciencemag.org/content/229/4716/857> doi: 10.1126/
 560 science.229.4716.857
- 561 Hansen, J., Sato, M., Ruedy, R., Nazarenko, L., Lacis, A., Schmidt, G. A., ...
 562 Zhang, S. (2005). Efficacy of climate forcings. *Journal of Geophysical*
 563 *Research: Atmospheres*, *110*(D18). Retrieved 2019-11-27, from [https://](https://agupubs.onlinelibrary.wiley.com/doi/abs/10.1029/2005JD005776)
 564 agupubs.onlinelibrary.wiley.com/doi/abs/10.1029/2005JD005776 doi:
 565 10.1029/2005JD005776
- 566 Haugstad, A. D., Armour, K. C., Battisti, D. S., & Rose, B. E. J. (2017).
 567 Relative roles of surface temperature and climate forcing patterns in
 568 the inconstancy of radiative feedbacks. *Geophysical Research Let-*
 569 *ters*, *44*(14), 7455–7463. Retrieved 2020-04-22, from [https://agupubs](https://agupubs.onlinelibrary.wiley.com/doi/abs/10.1002/2017GL074372)
 570 [.onlinelibrary.wiley.com/doi/abs/10.1002/2017GL074372](https://agupubs.onlinelibrary.wiley.com/doi/abs/10.1002/2017GL074372) (eprint:
 571 <https://agupubs.onlinelibrary.wiley.com/doi/pdf/10.1002/2017GL074372>) doi:
 572 10.1002/2017GL074372

- 573 Heydt, A. S. v. d., Dijkstra, H. A., Wal, R. S. W. v. d., Caballero, R., Crucifix, M.,
574 Foster, G. L., ... Ziegler, M. (2016). Lessons on Climate Sensitivity From
575 Past Climate Changes. *Current Climate Change Reports*, 2(4), 148–158. Re-
576 trieved 2019-12-19, from [https://link.springer.com/article/10.1007/
577 s40641-016-0049-3](https://link.springer.com/article/10.1007/s40641-016-0049-3) doi: 10.1007/s40641-016-0049-3
- 578 Hoffman, P. F., Kaufman, A. J., Halverson, G. P., & Schrag, D. P. (1998). A Neo-
579 proterozoic Snowball Earth. *Science*, 281(5381), 1342–1346. Retrieved 2019-
580 12-19, from <https://science.sciencemag.org/content/281/5381/1342>
581 doi: 10.1126/science.281.5381.1342
- 582 Ingersoll, A. P. (1969). The Runaway Greenhouse: A History of Water on
583 Venus. *Journal of the Atmospheric Sciences*, 26(6), 1191–1198. Re-
584 trieved 2019-12-19, from [https://journals.ametsoc.org/doi/abs/
585 10.1175/1520-0469%281969%29026%3C1191%3ATRGAHO%3E2.0.CO%3B2](https://journals.ametsoc.org/doi/abs/10.1175/1520-0469%281969%29026%3C1191%3ATRGAHO%3E2.0.CO%3B2) doi:
586 10.1175/1520-0469(1969)026<1191:TRGAHO>2.0.CO;2
- 587 Jonko, A. K., Shell, K. M., Sanderson, B. M., & Danabasoglu, G. (2013). Cli-
588 mate Feedbacks in CCSM3 under Changing CO₂ Forcing. Part II: Variation of
589 Climate Feedbacks and Sensitivity with Forcing. *Journal of Climate*, 26(9),
590 2784–2795. Retrieved 2019-11-27, from [https://journals.ametsoc.org/doi/
591 full/10.1175/JCLI-D-12-00479.1](https://journals.ametsoc.org/doi/full/10.1175/JCLI-D-12-00479.1) doi: 10.1175/JCLI-D-12-00479.1
- 592 Kamae, Y., Watanabe, M., Ogura, T., Yoshimori, M., & Shiogama, H. (2015).
593 Rapid Adjustments of Cloud and Hydrological Cycle to Increasing
594 CO₂: a Review. *Current Climate Change Reports*,
595 1(2), 103–113. Retrieved 2018-08-01, from [https://link.springer.com/
596 article/10.1007/s40641-015-0007-5](https://link.springer.com/article/10.1007/s40641-015-0007-5) doi: 10.1007/s40641-015-0007-5
- 597 Knutti, R., Rugenstein, M. A. A., & Hegerl, G. C. (2017). Beyond equilibrium cli-
598 mate sensitivity. *Nature Geoscience*, 10(10), 727–736. Retrieved 2018-11-01,
599 from <https://www.nature.com/articles/ngeo3017> doi: 10.1038/ngeo3017
- 600 Köhler, P., Stap, L. B., von der Heydt, A. S., de Boer, B., van de Wal, R. S. W.,
601 & Bloch-Johnson, J. (2017). A State-Dependent Quantification of Climate
602 Sensitivity Based On Paleodata of the Last 2.1 Million Years. *Paleoceanogra-
603 phy*, 32, 1102–1114. Retrieved 2018-06-28, from [http://doi.org/10.1002/
604 2017PA003190](http://doi.org/10.1002/2017PA003190) doi: 10.1002/2017PA003190
- 605 Koll, D. D. B., & Cronin, T. W. (2018, October). Earths outgoing longwave radia-
606 tion linear due to H₂O greenhouse effect. *Proceedings of the National Academy
607 of Sciences*, 115(41), 10293–10298. Retrieved 2019-09-30, from [https://www
608 .pnas.org/content/115/41/10293](https://www.pnas.org/content/115/41/10293) doi: 10.1073/pnas.1809868115
- 609 Komabayasi, M. (1967). Discrete Equilibrium Temperatures of a Hypothetical
610 Planet with the Atmosphere and the Hydrosphere of One Component-Two
611 Phase System under Constant Solar Radiation. *Journal of the Meteorological
612 Society of Japan. Ser. II*, 45(1), 137–139. doi: 10.2151/jmsj1965.45.1.137
- 613 Kutzbach, J. E., He, F., Vavrus, S. J., & Ruddiman, W. F. (2013). The dependence
614 of equilibrium climate sensitivity on climate state: Applications to studies of
615 climates colder than present. *Geophysical Research Letters*, 40(14), 3721–3726.
616 Retrieved 2019-12-19, from [https://agupubs.onlinelibrary.wiley.com/
617 doi/abs/10.1002/grl.50724](https://agupubs.onlinelibrary.wiley.com/doi/abs/10.1002/grl.50724) doi: 10.1002/grl.50724
- 618 Martínez-Botí, M. A., Foster, G. L., Chalk, T. B., Rohling, E. J., Sexton, P. F.,
619 Lunt, D. J., ... Schmidt, D. N. (2015). Plio-Pleistocene climate sensitivity
620 evaluated using high-resolution CO₂ records. *Nature*, 518(7537), 49–54. Re-
621 trieved 2019-12-20, from <https://www.nature.com/articles/nature14145>
622 doi: 10.1038/nature14145
- 623 Meraner, K., Mauritsen, T., & Voigt, A. (2013). Robust increase in equilibrium cli-
624 mate sensitivity under global warming. *Geophysical Research Letters*, 40(22),
625 5944–5948. Retrieved 2019-11-27, from [https://agupubs.onlinelibrary
626 .wiley.com/doi/abs/10.1002/2013GL058118](https://agupubs.onlinelibrary.wiley.com/doi/abs/10.1002/2013GL058118) doi: 10.1002/2013GL058118
- 627 Myhre, G., Highwood, E. J., Shine, K. P., & Stordal, F. (1998). New esti-

- 628 mates of radiative forcing due to well mixed greenhouse gases. *Geophys-*
 629 *ical Research Letters*, 25(14), 2715–2718. Retrieved 2020-01-10, from
 630 <https://agupubs.onlinelibrary.wiley.com/doi/abs/10.1029/98GL01908>
 631 doi: 10.1029/98GL01908
- 632 Pierrehumbert, R. T. (2013, August). Hot climates, high sensitivity. *Proceedings of*
 633 *the National Academy of Sciences*, 110(35), 14118–14119. Retrieved 2018-10-
 634 31, from <http://www.pnas.org/content/110/35/14118> doi: 10.1073/pnas
 635 .1313417110
- 636 Pincus, R., Forster, P. M., & Stevens, B. (2016, September). The Radiative Forcing
 637 Model Intercomparison Project (RFMIP): experimental protocol for CMIP6.
 638 *Geoscientific Model Development*, 9(9), 3447–3460. Retrieved 2020-04-23, from
 639 <https://www.geosci-model-dev.net/9/3447/2016/> (Publisher: Copernicus
 640 GmbH) doi: <https://doi.org/10.5194/gmd-9-3447-2016>
- 641 Rieger, V. S., Dietmiller, S., & Ponater, M. (2017). Can feedback analysis be used to
 642 uncover the physical origin of climate sensitivity and efficacy differences? *Cli-*
 643 *mate Dynamics*, 49(7), 2831–2844. Retrieved 2019-11-27, from [https://doi](https://doi.org/10.1007/s00382-016-3476-x)
 644 [.org/10.1007/s00382-016-3476-x](https://doi.org/10.1007/s00382-016-3476-x) doi: 10.1007/s00382-016-3476-x
- 645 Roe, G. H., & Armour, K. C. (2011, July). How sensitive is climate sensitivity?
 646 *Geophysical Research Letters*, 38(14). Retrieved 2018-10-31, from [https://](https://agupubs.onlinelibrary.wiley.com/doi/abs/10.1029/2011GL047913)
 647 agupubs.onlinelibrary.wiley.com/doi/abs/10.1029/2011GL047913 doi:
 648 10.1029/2011GL047913
- 649 Rohrschneider, T., Stevens, B., & Mauritsen, T. (2019). On simple representa-
 650 tions of the climate response to external radiative forcing. *Climate Dynamics*,
 651 53(5), 3131–3145. Retrieved 2019-11-27, from [https://doi.org/10.1007/](https://doi.org/10.1007/s00382-019-04686-4)
 652 [s00382-019-04686-4](https://doi.org/10.1007/s00382-019-04686-4) doi: 10.1007/s00382-019-04686-4
- 653 Rose, B. E. J., Armour, K. C., Battisti, D. S., Feldl, N., & Koll, D. D. B. (2014).
 654 The dependence of transient climate sensitivity and radiative feedbacks on the
 655 spatial pattern of ocean heat uptake. *Geophysical Research Letters*, 41(3),
 656 1071–1078. Retrieved 2018-06-28, from [https://agupubs.onlinelibrary](https://agupubs.onlinelibrary.wiley.com/doi/abs/10.1002/2013GL058955)
 657 [.wiley.com/doi/abs/10.1002/2013GL058955](https://agupubs.onlinelibrary.wiley.com/doi/abs/10.1002/2013GL058955) doi: 10.1002/2013GL058955
- 658 Rugenstein, M., Bloch-Johnson, J., Abe-Ouchi, A., Andrews, T., Beyerle, U.,
 659 Cao, L., ... Yang, S. (2019). LongRunMIP motivation and design
 660 for a large collection of millennial-length AO-GCM simulations. *Bul-*
 661 *letin of the American Meteorological Society*. Retrieved 2019-11-27, from
 662 <https://journals.ametsoc.org/doi/abs/10.1175/BAMS-D-19-0068.1> doi:
 663 10.1175/BAMS-D-19-0068.1
- 664 Rugenstein, M., Bloch-Johnson, J., Gregory, J., Andrews, T., Mauritsen, T., Li, C.,
 665 ... Knutti, R. (2020). Equilibrium climate sensitivity estimated by equili-
 666 brating climate models. *Geophysical Research Letters*, n/a(n/a). Retrieved
 667 2019-11-27, from [https://agupubs.onlinelibrary.wiley.com/doi/abs/](https://agupubs.onlinelibrary.wiley.com/doi/abs/10.1029/2019GL083898)
 668 [10.1029/2019GL083898](https://agupubs.onlinelibrary.wiley.com/doi/abs/10.1029/2019GL083898) doi: 10.1029/2019GL083898
- 669 Rugenstein, M., Gregory, J. M., Schaller, N., Sedlek, J., & Knutti, R. (2016).
 670 Multiannual OceanAtmosphere Adjustments to Radiative Forcing. *Jour-*
 671 *nal of Climate*, 29(15), 5643–5659. Retrieved 2018-08-01, from [https://](https://journals.ametsoc.org/doi/full/10.1175/JCLI-D-16-0312.1)
 672 journals.ametsoc.org/doi/full/10.1175/JCLI-D-16-0312.1 doi:
 673 10.1175/JCLI-D-16-0312.1
- 674 Seeley, J., & Jeevanjee, N. (2020, August). *H2O windows and CO2 radiator fins:*
 675 *a clear-sky explanation for the peak in ECS* [preprint]. Retrieved 2020-08-28,
 676 from <http://www.essoar.org/doi/10.1002/essoar.10503539.1> (Archive
 677 Location: world Publisher: Earth and Space Science Open Archive Section:
 678 Atmospheric Sciences) doi: 10.1002/essoar.10503539.1
- 679 Senior, C. A., & Mitchell, J. F. B. (2000). The time-dependence of climate sensi-
 680 tivity. *Geophysical Research Letters*, 27(17), 2685–2688. Retrieved 2018-06-
 681 28, from [https://agupubs.onlinelibrary.wiley.com/doi/abs/10.1029/](https://agupubs.onlinelibrary.wiley.com/doi/abs/10.1029/2000GL011373)
 682 [2000GL011373](https://agupubs.onlinelibrary.wiley.com/doi/abs/10.1029/2000GL011373) doi: 10.1029/2000GL011373

- 683 Shaffer, G., Huber, M., Rondanelli, R., & Pedersen, J. O. P. (2016). Deep time
684 evidence for climate sensitivity increase with warming. *Geophysical Re-*
685 *search Letters*, *43*(12), 6538–6545. Retrieved 2018-05-15, from [https://](https://agupubs.onlinelibrary.wiley.com/doi/abs/10.1002/2016GL069243)
686 agupubs.onlinelibrary.wiley.com/doi/abs/10.1002/2016GL069243 doi:
687 10.1002/2016GL069243
- 688 Sherwood, S. C., Bony, S., Boucher, O., Bretherton, C., Forster, P. M., Gre-
689 gory, J. M., & Stevens, B. (2014). Adjustments in the Forcing-Feedback
690 Framework for Understanding Climate Change. *Bulletin of the Ameri-*
691 *can Meteorological Society*, *96*(2), 217–228. Retrieved 2018-08-01, from
692 <https://journals.ametsoc.org/doi/abs/10.1175/BAMS-D-13-00167.1>
693 doi: 10.1175/BAMS-D-13-00167.1
- 694 Sherwood, S. C., Webb, M. J., Annan, J. D., Armour, K. C., Forster, P. M., Har-
695 greaves, J. C., ... Zelinka, M. D. (2020). An assessment of Earth’s cli-
696 mate sensitivity using multiple lines of evidence. *Reviews of Geophysics*,
697 *n/a*(n/a), e2019RG000678. Retrieved 2020-09-15, from [https://agupubs](https://agupubs.onlinelibrary.wiley.com/doi/abs/10.1029/2019RG000678)
698 [.onlinelibrary.wiley.com/doi/abs/10.1029/2019RG000678](https://agupubs.onlinelibrary.wiley.com/doi/abs/10.1029/2019RG000678) (eprint:
699 <https://agupubs.onlinelibrary.wiley.com/doi/pdf/10.1029/2019RG000678>) doi:
700 10.1029/2019RG000678
- 701 Smith, C. J., Kramer, R. J., Myhre, G., Alberskjær, K., Collins, W., Sima, A., ...
702 Forster, P. M. (2020, January). Effective radiative forcing and adjustments
703 in CMIP6 models. *Atmospheric Chemistry and Physics Discussions*, 1–37.
704 Retrieved 2020-04-23, from [https://www.atmos-chem-phys-discuss.net/](https://www.atmos-chem-phys-discuss.net/acp-2019-1212/)
705 [acp-2019-1212/](https://www.atmos-chem-phys-discuss.net/acp-2019-1212/) (Publisher: Copernicus GmbH) doi: [https://doi.org/](https://doi.org/10.5194/acp-2019-1212)
706 [10.5194/acp-2019-1212](https://doi.org/10.5194/acp-2019-1212)
- 707 Snyder, C. W. (2019, September). Revised estimates of paleoclimate sensitivity over
708 the past 800,000 years. *Climatic Change*, *156*(1), 121–138. Retrieved 2020-
709 04-03, from <https://doi.org/10.1007/s10584-019-02536-0> doi: 10.1007/
710 [s10584-019-02536-0](https://doi.org/10.1007/s10584-019-02536-0)
- 711 Soden, B. J., Broccoli, A. J., & Hemler, R. S. (2004, October). On the Use of Cloud
712 Forcing to Estimate Cloud Feedback. *Journal of Climate*, *17*(19), 3661–3665.
713 Retrieved 2018-06-28, from [https://journals.ametsoc.org/doi/full/](https://journals.ametsoc.org/doi/full/10.1175/1520-0442%282004%29017%3C3661:OTUOCF%3E2.0.CO%3B2)
714 [10.1175/1520-0442%282004%29017%3C3661:OTUOCF%3E2.0.CO%3B2](https://journals.ametsoc.org/doi/full/10.1175/1520-0442%282004%29017%3C3661:OTUOCF%3E2.0.CO%3B2) doi:
715 [10.1175/1520-0442\(2004\)017\(3661:OTUOCF\)2.0.CO;2](https://doi.org/10.1175/1520-0442(2004)017(3661:OTUOCF)2.0.CO;2)
- 716 Stocker, T. F., Qin, D., Plattner, G.-K., Tignor, M., Allen, S., Boschung, J.,
717 ... Midgley, P. (2013). *AR5 Climate Change 2013: The Physical Sci-*
718 *ence Basis IPCC* (Tech. Rep.). Cambridge, United Kingdom and New
719 York, NY, USA: Cambridge University Press. Retrieved 2019-12-19, from
720 <https://www.ipcc.ch/report/ar5/wg1/>
- 721 Stolpe, M. B., Medhaug, I., Beyerle, U., & Knutti, R. (2019). Weak dependence of
722 future global mean warming on the background climate state. *Climate Dynam-*
723 *ics*, *53*(7), 5079–5099. Retrieved 2019-11-27, from [https://doi.org/10.1007/](https://doi.org/10.1007/s00382-019-04849-3)
724 [s00382-019-04849-3](https://doi.org/10.1007/s00382-019-04849-3) doi: 10.1007/s00382-019-04849-3
- 725 Stouffer, R. J., & Manabe, S. (2003). Equilibrium response of thermohaline cir-
726 culation to large changes in atmospheric CO₂ concentration. *Climate Dynam-*
727 *ics*, *20*(7), 759–773. Retrieved 2019-11-27, from [https://doi.org/10.1007/](https://doi.org/10.1007/s00382-002-0302-4)
728 [s00382-002-0302-4](https://doi.org/10.1007/s00382-002-0302-4) doi: 10.1007/s00382-002-0302-4
- 729 Tan, I., Storelvmo, T., & Zelinka, M. D. (2016, April). Observational constraints on
730 mixed-phase clouds imply higher climate sensitivity. *Science*, *352*(6282), 224–
731 227. Retrieved 2020-04-24, from [https://science.sciencemag.org/content/](https://science.sciencemag.org/content/352/6282/224)
732 [352/6282/224](https://science.sciencemag.org/content/352/6282/224) (Publisher: American Association for the Advancement of Sci-
733 ence Section: Report) doi: 10.1126/science.aad5300
- 734 Taylor, K. E., Crucifix, M., Braconnot, P., Hewitt, C. D., Doutriaux, C., Broc-
735 coli, A. J., ... Webb, M. J. (2007, June). Estimating Shortwave Radiative
736 Forcing and Response in Climate Models. *Journal of Climate*, *20*(11), 2530–
737 2543. Retrieved 2020-03-08, from <https://journals.ametsoc.org/doi/>

- 738 10.1175/JCLI4143.1 (Publisher: American Meteorological Society) doi:
 739 10.1175/JCLI4143.1
- 740 Valdes, P. (2011). Built for stability. *Nature Geoscience*, 4(7), 414–416. Re-
 741 trieved 2020-01-06, from <https://www.nature.com/articles/ngeo1200> doi:
 742 10.1038/ngeo1200
- 743 Winton, M., Adcroft, A., Dunne, J. P., Held, I. M., Shevliakova, E.,
 744 Zhao, M., ... Zhang, R. (2020). Climate Sensitivity of GFDL’s
 745 CM4.0. *Journal of Advances in Modeling Earth Systems*, 12(1),
 746 e2019MS001838. Retrieved 2020-04-22, from [https://agupubs](https://agupubs.onlinelibrary.wiley.com/doi/abs/10.1029/2019MS001838)
 747 [.onlinelibrary.wiley.com/doi/abs/10.1029/2019MS001838](https://agupubs.onlinelibrary.wiley.com/doi/abs/10.1029/2019MS001838) (eprint:
 748 <https://agupubs.onlinelibrary.wiley.com/doi/pdf/10.1029/2019MS001838>) doi:
 749 10.1029/2019MS001838
- 750 Wolf, E. T., HaqqMisra, J., & Toon, O. B. (2018). Evaluating Climate Sensitivity
 751 to CO₂ Across Earth’s History. *Journal of Geophysical Research: Atmo-*
 752 *spheres*, 123(21), 11,861–11,874. Retrieved 2020-04-21, from [https://agupubs](https://agupubs.onlinelibrary.wiley.com/doi/abs/10.1029/2018JD029262)
 753 [.onlinelibrary.wiley.com/doi/abs/10.1029/2018JD029262](https://agupubs.onlinelibrary.wiley.com/doi/abs/10.1029/2018JD029262) (eprint:
 754 <https://agupubs.onlinelibrary.wiley.com/doi/pdf/10.1029/2018JD029262>) doi:
 755 10.1029/2018JD029262
- 756 Yoshimori, M., Yokohata, T., & Abe-Ouchi, A. (2009). A Comparison of Cli-
 757 mate Feedback Strength between CO₂ Doubling and LGM Experiments.
 758 *Journal of Climate*, 22(12), 3374–3395. Retrieved 2019-09-28, from
 759 <https://journals.ametsoc.org/doi/full/10.1175/2009JCLI2801.1> doi:
 760 10.1175/2009JCLI2801.1
- 761 Zaliapin, I., & Ghil, M. (2010, March). Another Look at Climate Sensitivity.
 762 *Nonlinear Processes in Geophysics*, 17(2), 113–122. Retrieved 2018-10-
 763 31, from <http://arxiv.org/abs/1003.0253> (arXiv: 1003.0253) doi:
 764 10.5194/npg-17-113-2010
- 765 Zhang, Y., Jeevanjee, N., & Fueglistaler, S. (2020). Linearity of
 766 Outgoing Longwave Radiation: From an Atmospheric Column to
 767 Global Climate Models. *Geophysical Research Letters*, 47(17),
 768 e2020GL089235. Retrieved 2020-11-20, from [https://agupubs](https://agupubs.onlinelibrary.wiley.com/doi/abs/10.1029/2020GL089235)
 769 [.onlinelibrary.wiley.com/doi/abs/10.1029/2020GL089235](https://agupubs.onlinelibrary.wiley.com/doi/abs/10.1029/2020GL089235) (eprint:
 770 <https://agupubs.onlinelibrary.wiley.com/doi/pdf/10.1029/2020GL089235>) doi:
 771 <https://doi.org/10.1029/2020GL089235>
- 772 Zhou, C., Zelinka, M. D., & Klein, S. A. (2017). Analyzing the dependence
 773 of global cloud feedback on the spatial pattern of sea surface temperature
 774 change with a Green’s function approach. *Journal of Advances in Model-*
 775 *ing Earth Systems*, 9(5), 2174–2189. Retrieved 2018-05-12, from [https://](https://agupubs.onlinelibrary.wiley.com/doi/full/10.1002/2017MS001096)
 776 agupubs.onlinelibrary.wiley.com/doi/full/10.1002/2017MS001096 doi:
 777 10.1002/2017MS001096
- 778 Zhu, J., Poulsen, C. J., & Tierney, J. E. (2019, September). Simulation of
 779 Eocene extreme warmth and high climate sensitivity through cloud feed-
 780 backs. *Science Advances*, 5(9), eaax1874. Retrieved 2019-12-21, from
 781 <https://advances.sciencemag.org/content/5/9/eaax1874> doi:
 782 10.1126/sciadv.aax1874